from: "Patch Dynamics", Levin, Steele and Powell, 1993 (149)

M 150.209 1492

13
# MECHANISMS OF PATCH FORMATION

Douglas H. Deutschman, Gay A. Bradshaw, W. Michael Childress, Kendra L. Daly, Daniel Grünbaum, Mercedes Pascual, Nathan H. Schumaker, and Jianguo Wu

## INTRODUCTION

Many mechanisms both physical (e.g., light, temperature, ocean currents, density gradients, topography) and biological (e.g., allelopathy, competition, predation, selective foraging) are considered responsible for patch formation. Wiens (1976) presented an excellent review of population responses to environmental patchiness. He identified localized random disturbances (e.g., fire, erosion, tree windfalls), predation, selective herbivory, and vegetational patterns as potential causes of patch formation. Roughgarden (1977) discussed five general mechanisms that are responsible for patchiness: resource distribution, dispersal, aggregation behavior, competition, and reaction-diffusion.

Patch-forming mechanisms operate at different spatial and temporal scales. Different mechanisms may predominate on one or more characteristic scales. For instance, fires are considered a dominant mechanism producing conspicuous patchiness at relatively large scales in many terrestrial systems (e.g., deciduous forests, grasslands). In contrast, vegetative propagation creates patchiness at relatively small scales. In marine plankton, reproductive population growth may dominate at large scales while behavioral adaptations of individuals tend to dominate at small scales. Further, the scale at which this transition occurs will vary with the size, longevity, and mobility of the organism (Mackas et al. 1985). Variability of environmental conditions (e.g., temperature) and the diversity of an organism's behavioral and physiological responses contribute to patchiness at many different scales in both terrestrial and marine systems (see Pickett and White 1985, Kolasa and Pickett 1991).

To understand the consequences of patchiness, we need to understand:

1) On what spatial and temporal scales do organisms respond to patches in their environment?

2) How do processes scale up and scale down?

3) How do simple patch-forming mechanisms interact in space and time to give rise to more complex patterns?

In this chapter, we present brief discussions of our attempts to integrate the scale of patch-forming processes. The first section focuses on the importance of identifying the characteristic scales of the organism and its environment in order to understand how organisms perceive and potentially react to patchiness. We address the question: What can be determined about small-scale (= high resolution) spatial patterns from large-scale (= low resolution) data such as satellite imagery and aerial photographs? Finally, we present an integrated empirical and theoretical investigation of the multiple scales over which patchiness is observed in the distribution of the Antarctic krill, *Euphausia superba*. This first section demonstrates the need to consider the implicit scales of the organism, the environment, and the data.

The second section is devoted to demonstrating how interactions of relatively simple processes can generate very complex patterns of patchiness. This is approached through the use of two different spatial simulation models. The first model examines the results of random movement interacting with predator-prey cycles on a one-dimensional gradient. In the second model, the environment consists of a two-dimensional array of cells of uniform quality. In both cases, the interaction of movement with the predator-prey dynamics leads to complex spatial patterns. While these studies reflect only a narrow range of possible examples, they demonstrate how both the scaling and the interactions of patch-forming mechanisms are critical to an understanding of patchiness.

## SCALE

### Relative Scales

Despite its prevalence in recent ecological literature, the definition of a patch has remained controversial. Early definitions distinguished a patch from spatial variability by its relatively discrete boundary and internal homogeneity (Levin and Paine 1974, Wiens 1976). Kotliar and Wiens (1990) stressed that a patch is simply a surface area differing from its surroundings and that patches form a hierarchical mosaic over a broad range of scales. In the marine context, this range of scales is portrayed as a continuum with methods like power spectra (Platt and Denman 1975). This dichotomy corresponds to the difference between terrestrial and aquatic patterns. Thus, it would not be fruitful to attempt a general definition of patchiness because patches cannot be defined in the abstract. They must be defined relative to the investigation in order to render the term meaningful (for more discussion, see the chapter by García-Moliner et al.).

Investigations into the role of patchiness must consider the spatial and temporal scales that are relevant to the organism under study (Steele 1978, Wiens and Milne 1989, Downes 1990). It is clear that a sessile organism will respond to phenomena at spatial scales quite distinct from those to which a motile organism responds. Similarly, the adult stage of an organism may experience vastly different environmental patches than a larva or juvenile of the same species. Insects that undergo metamorphosis and benthic organisms with pelagic larvae are extreme examples of this phenomenon. Other features of an organism's life history such as size, dispersal, dormancy, and foraging strategies will affect its perception of scales.

Addicott et al. (1987) formalized the notion of relevant scales with the definition of "ecological neighborhoods." The ecological neighborhood is defined in three sequential steps: 1) choosing the organism; 2) identifying the ecological process; and 3) determining the appropriate temporal and spatial scales. This approach has a graphical analog similar to the

Stommel diagram (Haury et al. 1978, after Stommel 1963; for more discussion see the chapter by Marquet et al.), which involves the generation of a log-log plot of the time and space components of the organism's ecological neighborhood (Figure 1a).

The graphical approach is useful in exploring interactions between a specific organism and its environment. Environmental events (e.g., seasonal and diel changes, disturbance) can be plotted onto the same axes (Figure 1b). Spatial scale indicates the range of the event, while the temporal scale is based on the frequency of the event. Predictable events (i.e., diel, lunar, seasonal, and annual) are indicated by discrete lines. Less predictable events are represented by confidence ellipses indicating the amount and direction of the spatial and temporal variability.

The position of these events relative to the organism will influence how the organism responds to each event (see Hutchinson 1961). Events occurring over spatial and temporal scales similar to those of the organism itself are likely to have the most pronounced effect. Processes that are larger in spatial or temporal extent than the organism's ecological neighborhood would not be experienced as patches or events by the organism; the effect would more likely be at the population level. Events occurring over smaller scales or shorter time period (below the "grain," *sensu* Kotliar and Wiens 1990) are often averaged out by the behavior and physiology of the organism.

## Resolving Small-scale Spatial Patterns and Processes from Large-scale Patterns: Grid-based Computer Simulations

Although comprehensive in extent, aerial and satellite imagery have fixed minimum resolutions well above the scales at which individual organisms can be resolved. Because many important ecological interactions occur below the pixel level, it is necessary to develop methods that can derive information about small-scale spatial processes and patterns from large-scale spatial patterns. Assuming that ecological processes at a particular scale can cause patterns at other (especially larger) scales, we consider the following question: What can be determined about high-resolution spatial patterns and processes from spatial patterns observed at lower resolutions? As a heuristic example, a two-dimensional grid cell spatial model is presented and used as a means to investigate the general relationships among spatial patterns in grids of different scales.

*Methods*. Grids and spatial patterns were generated using computer simulations similar to those in Milne (1991). Each high-resolution grid was a 100 x 100 cell matrix wherein each cell could be in one of two states, ON or OFF. These binary states are considered equivalent to the presence or absence of an individual organism at a particular location in a given landscape. Different grids were generated in which the proportion $f$ of ON cells varied from 0.05 to 0.95, and the location of ON cells across the grid was random, clustered, or dispersed.

The initial high-resolution grid was generated in a two-step procedure, beginning with an initial scan of the grid to "seed" the ON cells. Here, 10% of the number of ON cells were placed at random in an empty grid. Subsequent scans and placement of ON cells were performed until the desired proportion of ON cells was achieved. In each scan and for each OFF cell, a random number was compared with $0.02fg^n$, where $g$ is an aggregation factor and $n$ is the number of neighboring cells (from 0 to 8) that are ON. This calculation allowed weighting the likelihood that a particular cell would be turned ON by the presence of other

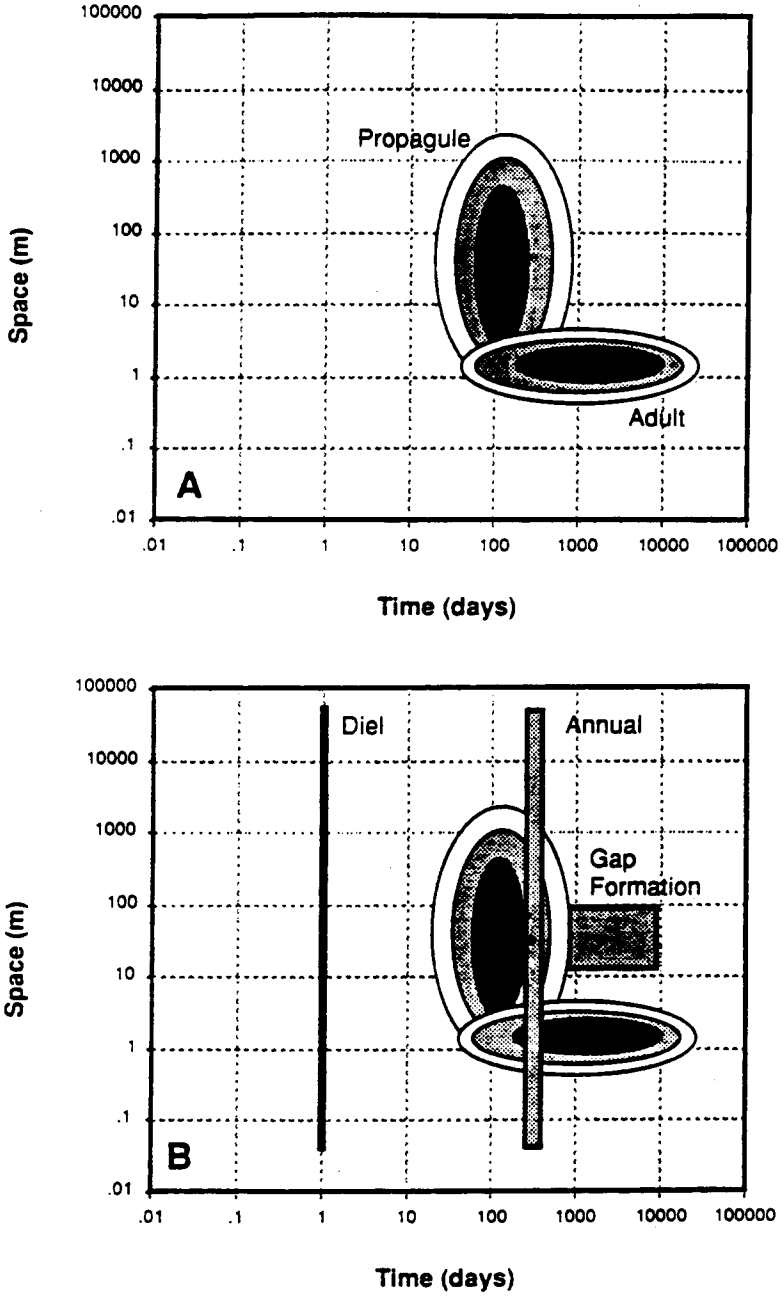


Figure 1. Diagram of the spatial and temporal scales for the propagule and adult stages of a hypothetical tree. (a) Shaded confidence ellipses show the variability in the "species." (b) Environmental processes that can affect tree growth and survival. Diel and annual environmental change occur across all spatial scales. Gap formation is more variable but has a characteristic frequency and size distribution.

ON cells: when $g = 1$, there is no effect of neighbors; when $g < 1$, the presence of neighboring ON cells decreases the probability of turning the cell ON; and when $g > 1$, the probability is increased by each ON neighbor. In this study, the amount of aggregation ($g$) was set at three different levels: 1 (random), 0.5 (spread), and 1.5 (clustered). By this procedure, random, spread, and clustered spatial patterns were generated. The coefficient 0.02 ensured that a number of scans (about 40 - 50) was conducted so that patterns were gradually built and the desired proportion of ON cells was not greatly overshot by the last scan.

Three lower-resolution grids (20 x 20, 10 x 10, and 5 x 5 total pixels) were derived from the 100 x 100 grid by combining blocks of cells. Separate 5 x 5 blocks of cells from the 100 x 100 grid were grouped to form a single cell in the 20 x 20 grid; 10 x 10 blocks were combined for each cell in the 10 x 10 grid; and 20 x 20 cell blocks made up each cell in the 5 x 5 grid. The state for the lower-resolution cells was determined by one of three methods:

a) Presence/Absence: if at least one of the cells in the aggregation block was ON, then the corresponding cell in the higher-level grid was turned ON.

b) 30% threshold: if at least 30% of the cells in the block were ON, then the corresponding cell was turned ON.

c) 50% threshold: if at least 50% of the cells in the block were ON, then the corresponding cell was turned ON.

Evaluations of relationships between lower- and higher-resolution grids were based on the proportion of ON cells and the spatial pattern in the 100 x 100 grid versus the proportion of ON cells in the lower-resolution grids.

*Results*. Three results are presented here.

1) For a random spatial pattern in the 100 x 100 grid, the proportion of ON cells in the three lower-resolution grids increased nonlinearly and at different rates with increase in the proportion of ON cells (Figure 2a). This particular result can be derived analytically. Since each cell is independent, the binomial distribution gives the probability of any group of cells having a certain proportion of ON cells.

2) The three different criteria used in determining the state of the cells in low-resolution grids caused significant displacements of these curves (Figure 2b).

3) As the required proportion of ON cells in the lower-resolution cell increased, the curve shifted to the right. There was little difference in the low-resolution grids for different spatial patterns (random, spread, or clustered) in the 100 x 100 grid (for an example, see Figure 2c).

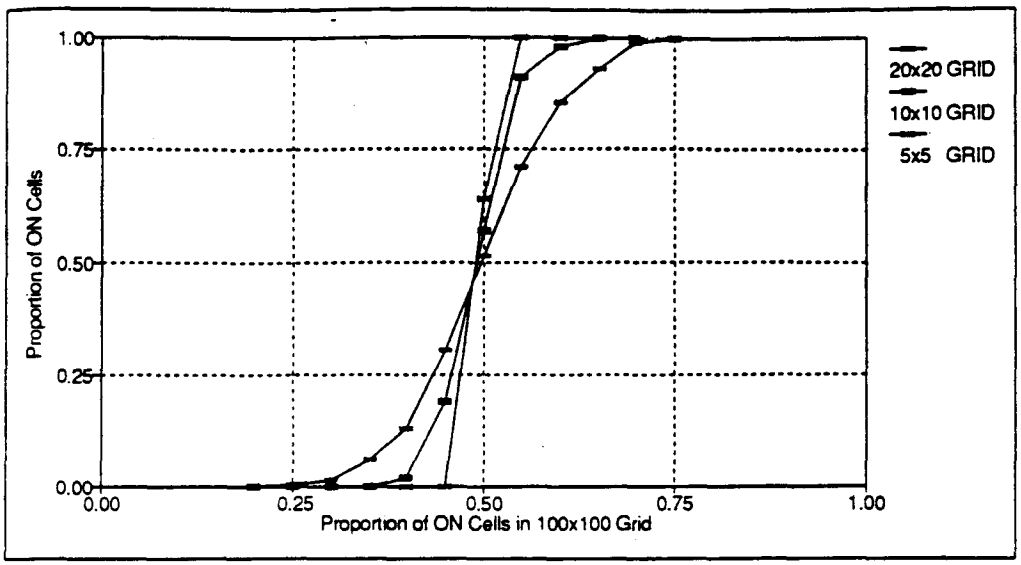


Figure 2a. Proportion of ON cells in the three higher-level aggregated grids at various proportions of ON cells in random pattern 100 x 100 low-level grid. The threshold criterion for aggregation of low-level cells to high-level cells was 50% ON in the cell block.

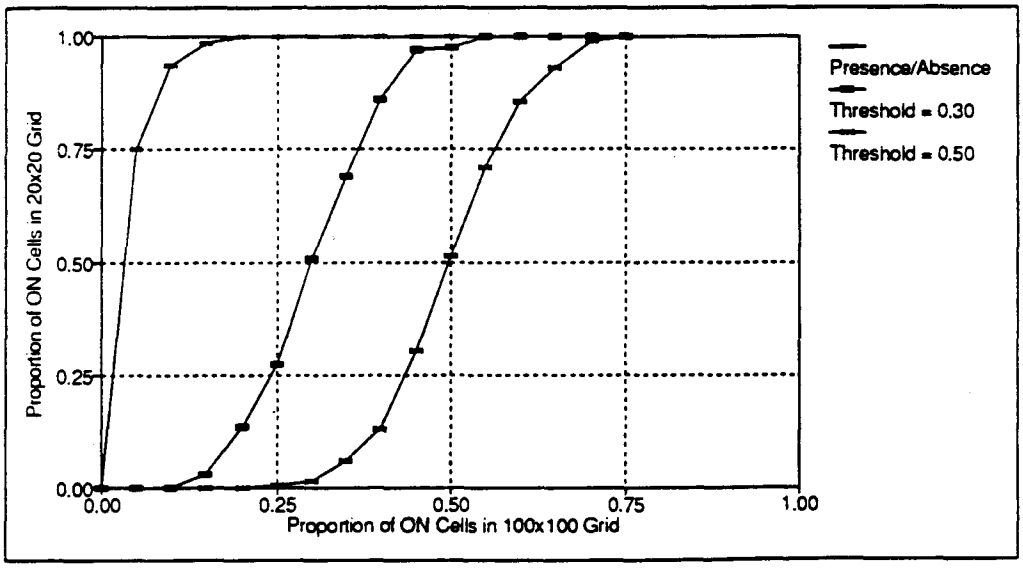


Figure 2b. Proportion of ON cells in the 20 x 20 cell grid using different criteria for aggregating low-level cell states into higher-level cell states. Cells in the low-level 100 x 100 grid were distributed in a random pattern.

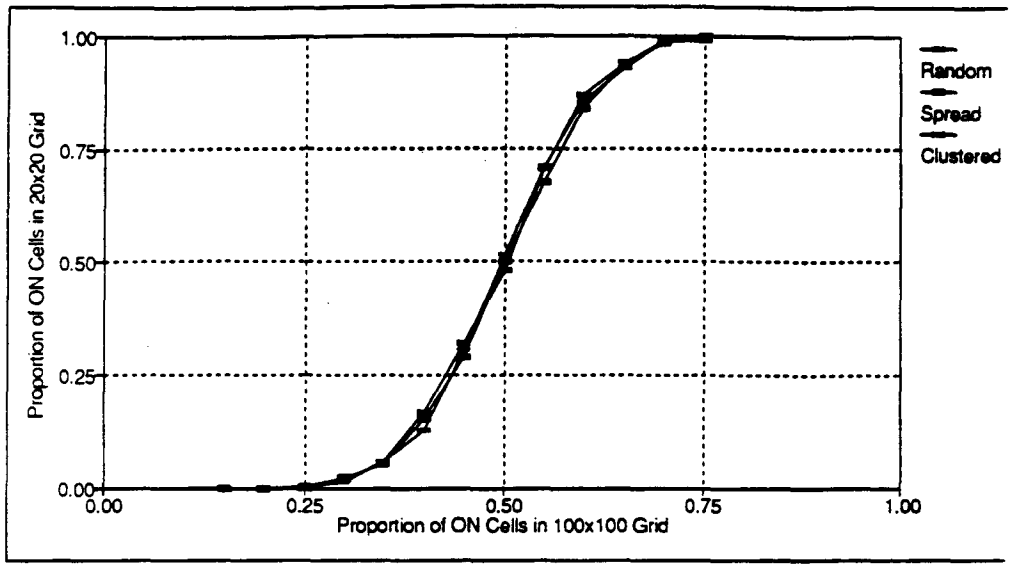


Figure 2c. Proportion of ON cells in the 20 x 20 grid for different spatial patterns of cells in the low-level 100 x 100 grid. The aggregation criterion was an ON threshold of 5 for cells in the aggregation block.

*Conclusions.* These results are both encouraging and disappointing. Fi low-resolution grids can apparently be used to estimate the proportion of ON cells higher-resolution grids. However, this requires some knowledge of how individual cell sta are combined into larger cells. Second, it appears that both the scales and the thresh criteria for low-resolution grids strongly affect the shape and location of curves express relationships between low- and high-resolution proportions of ON cells. Third, there v little difference in low-resolution ON proportion curves among random, spread, and cluster patterns in the original 100 x 100 grid, indicating there is apparently little disciminating pov for high-resolution spatial pattern in this approach. On the other hand, this may show t the approach is a fairly robust indication of the proportion of ON cells in the high-resolut grid, regardless of their pattern.

A number of research questions and directions are indicated by this preliminary effc In satellite data, aggregation of pixels is commonly used to resolve huge data streams in b terrestrial and marine imagery. The use of two-dimensional grid models is now comm Thus the relationship of these image-processing techniques to patch dynamic simulations worth further study.

Multiscale Patterns: Modeling and Empirical Data on Krill Aggregations

Spatial patchiness in physical and biological phenomena has been observed at virtually every scale investigated (Haury et al. 1978, Steele 1978), but little is known about the roles of physical vs. biological or induced vs. autonomous mechanisms that cause heterogeneity. Analytical techniques that elucidate the predominance or interactions of these mechanisms, therefore, are urgently needed.

We compare the results of analyses of field data from the Southern Ocean using two techniques: spectral analysis, a method often applied in marine systems (e.g., Platt and Denman 1975), and wavelet analysis, a relatively new statistical procedure recently applied to ecological and physical data (Argoul et al. 1989, Bradshaw 1991, Bradshaw and Spies, in press). The wavelet analysis is an alternative method for quantifying spatial pattern. These methods are employed in the present analysis to examine the characteristic scales of variability of a physical property (temperature), primary production (chlorophyll fluorescence), and an important herbivore (the Antarctic krill, *Euphausia superba*) in order to develop hypotheses about mechanisms that generate multi-scale patterns (see the chapter by García-Moliner et al. for a description of wavelet analysis).

Previous Antarctic investigations have concluded that observed variability in phytoplankton distribution is governed primarily by physical processes, because the power spectra of temperature and chlorophyll were consistent with those of passively advected scalars (Weber et al. 1986, Levin et al. 1989). In contrast, the spectra of krill biomass distribution showed greater variability at small spatial scales than those of temperature and phytoplankton. We hypothesize that this difference arises, in part, from the social behavior of krill, and we examine this hypothesis with the use of a model of an idealized aggregating species (Grünbaum 1991). Results from both the field data and the model suggest that behavior is an important mechanism contributing to the heterogeneous distribution of krill at small scales.

*E. superba* is an important link in the Antarctic marine food web and also the subject of a commercial fishery. On the scale of this large marine ecosystem, the spatial patterns of krill are probably controlled primarily by physical processes (Sahrhage 1988). On smaller scales, however, biological factors including behavior may influence krill spatial patterns (Price et al. 1988, Daly and Macaulay 1991).

*Methods*. Sea-surface temperature and chlorophyll-*a* fluorescence (provided by O. Holm-Hansen and W. Helbling, Scripps Institution of Oceanography; and A. Amos, University of Texas at Austin) and vertically integrated acoustic biomass of krill (provided by M. C. Macaulay, University of Washington) were collected along a 120 km transect north of Elephant Island near the Antarctic Peninsula during two surveys, approximately one month apart, in mid-summer (Rosenberg and Hewitt 1991).

In the present study, we analyzed temperature, chlorophyll, and acoustic biomass data to identify possible spatial relationships between krill and physical-biological factors by determining (1) the characteristic distances over which significant changes in each variable occurred, and (2) the spatial correlation among the three variables. The sampling resolution was 100 m for acoustic data and 800 m for temperature and chlorophyll data. Thus, the smallest scale compared for correlation analyses was 800 m (These scales complement the analysis of krill data in the chapter by García-Moliner et al.).

*Field Results*. The field data showed spatial patterns typical of other results (e. Mackas et al. 1985, Weber et al. 1986). Sea-surface temperature showed little structure a changed gradually with distance; chlorophyll was similar but showed more spatial pattern; a krill density showed complex spatial structure (Figure 3). The spatial pattern of krill also w not uniform along the transect; patch size and abundance varied with location. The pow spectra were similar to those of Weber et al. (1986) and indicated that the distribution of kr on both transects was highly variable at spatial scales smaller then 1000 m. The wave transform revealed that all three variables had spatial structure at different scales. Sea-surfa temperature (Figure 4a) and chlorophyll concentration (Figure 4b) each had one characteris scale, ca. 15 km and 5 - 10 km, respectively, while krill distribution (Figures 4c,d) w characterized by patches on several scales, ca. 25 km, 10 km, and < 200m. These patch had a hierarchical structure, with fine-scale features nested in larger features, as shown by t increasing complexity of structure and detail from large (Figure 4c) to small scales (Figu 4d). The special feature of the wavelet method is to display locational information. Wave analysis indicated that krill were aggregated into three large patches along the transect, 2 25 km in width; that there were few krill between 30 - 45 km; and that fine-scale structu was less pronounced between 0 - 10 and 100 - 120 km (Figures 3 and 4c).

Wavelet cross-covariance analysis did not indicate a strong association between a of the variables at zero lag. The spatial patterns of temperature and chlorophyll, howev were associated with an offset of 2 km (Figure 5a). In other words, 10 km patches relatively high phytoplankton density were offset by 2 km from 10 km patches of co temperature water. Chlorophyll and krill distributions also were negatively correlated a scale of about 20 km, with an offset of 4 km (Figure 5b).

*Model Results*. To provide additional insight for understanding spatial patterns of kri a model of an idealized aggregating species is used to examine the qualitative effects schooling or swarming behavior on spatial distribution and spectral density. This continuu model of density-dependent aggregation is derived directly from a stochastic model aggregating individuals (Grünbaum 1991).

In the stochastic model, individuals form aggregations by swimming toward or aw from neighbors in search of a desired "target" density. The premise of the model is th aggregating individuals make decisions on the direction in which to move based on a limit amount of information about the distribution of other individuals around them. This limitati is incorporated in the model in the form of a "sensing range," the distance at whi individuals can detect one another. Movement based on density-dependent decisions can on be in response to a sample of neighbors within this range. Instantaneous measurements of th relatively small number of individuals, therefore, are random quantities, which on statistically describe the average local population density and density gradient.

The response of a species to a continuously forcing velocity field can be compared the presence and absence of aggregation behavior. To make this comparison as explicit possible, it is convenient to have a velocity field that has a single characteristic length scal One possible choice of such a velocity field is simply a traveling sine wave. At any positic this velocity field results in a succession of converging and diverging velocity fields.

A comparison between the density distributions and the spectra of aggregating ar non-aggregating species for a typical choice of parameters is shown in Figure 6. Here, th characteristic length scale of the velocity perturbation is much larger than the sensing distanc The density distribution (Figure 6a) of the non-aggregating species shows variation primari

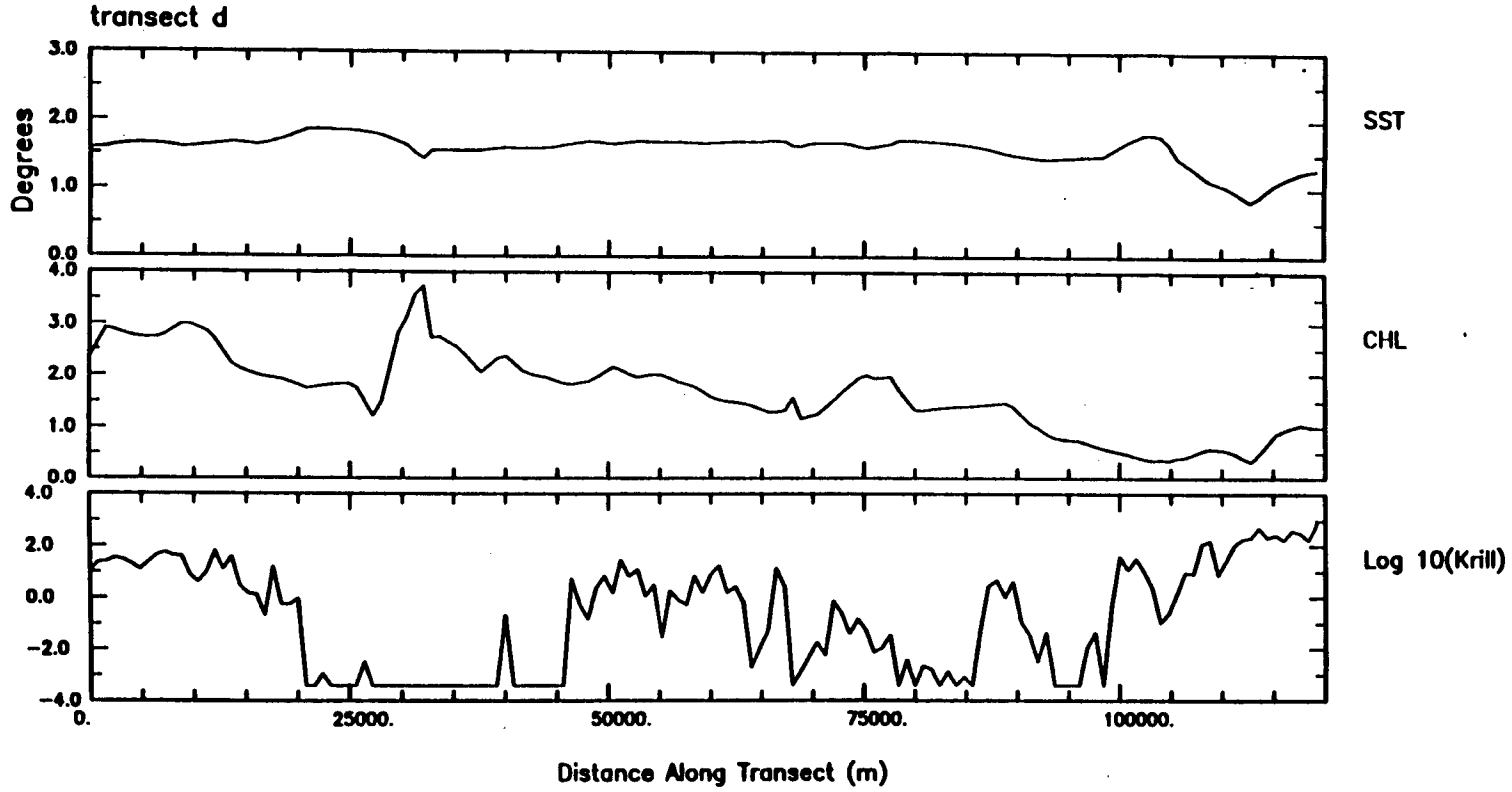


Figure 3. Field data for transect d illustrating different spatial patterns for sea-surface temperature (SST, °C) and chlorophyll-*a* concentration (CHL, mg $l^{-1}$), and acoustic biomass of krill integrated 6 - 250 m ($\log_{10}$ krill, g $m^{-2}$). X-axis denotes distance along the transect in meters; transect runs approximately west to east.

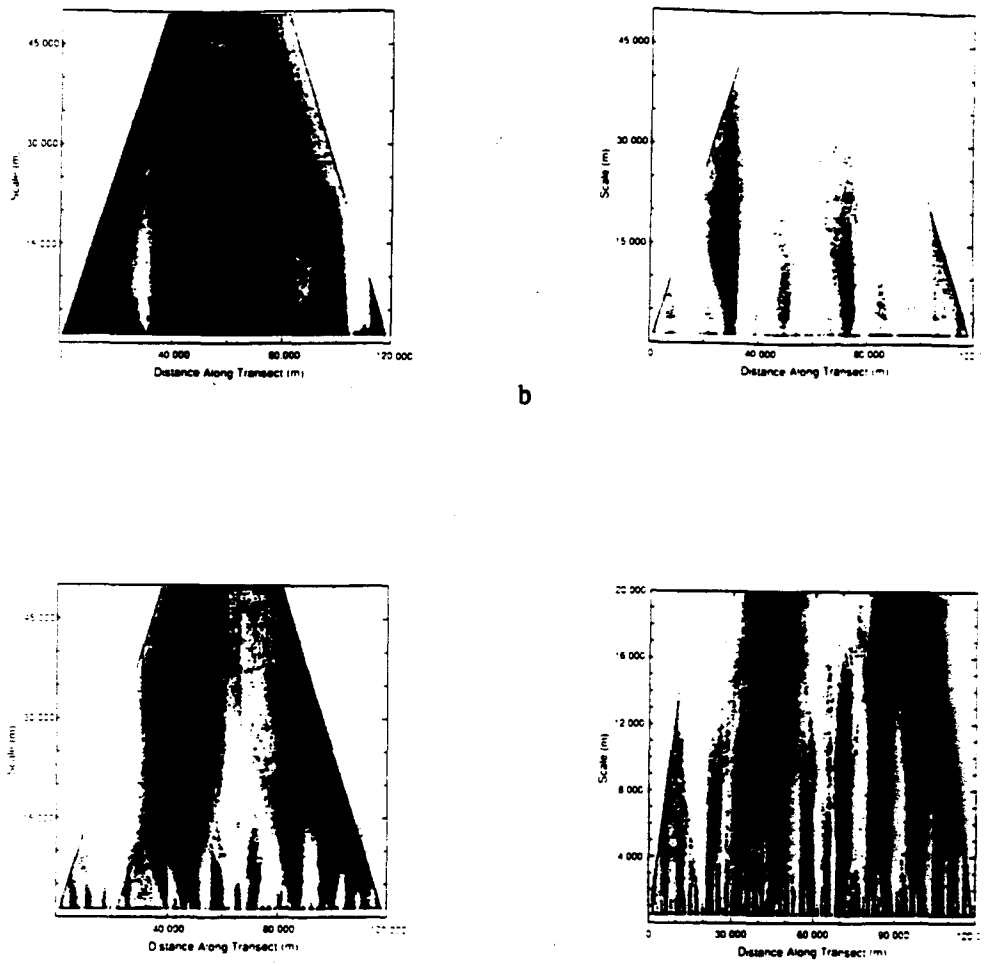


Figure 4. The wavelet transform calculated for: (a) sea-surface temperature data; (b) chlorophyll data; (c) krill data at the same scale as temperature and chlorophyll; (d) krill data at a finer scale (100 - 20,000 m; note the presence of features at several scales). The wavelet transform coefficients have been interpolated; dark shading corresponds to low values in the data and light shading corresponds to higher values in the data. View the figure near-parallel to plane of the page to facilitate detection of across-scale structure.

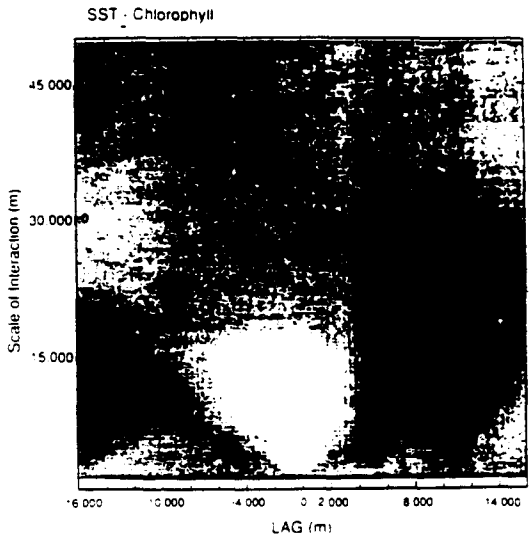


a

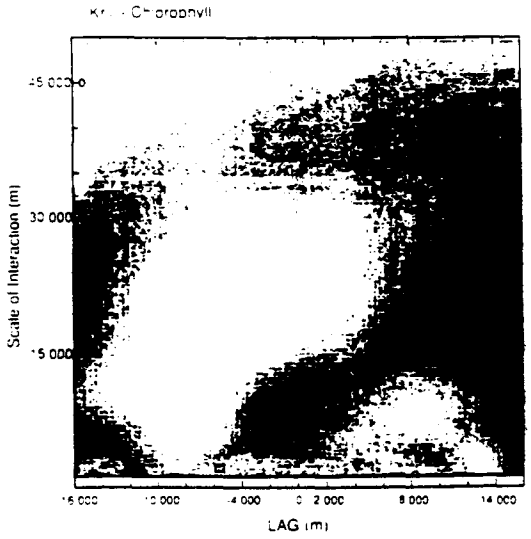


b

Figure 5. The wavelet cross-covariance function for: (a) sea-surface temperature; (b) chlorophyll. The grey-scale bar at the base of the figure identifies the magnitude of the wavelet cross-covariance; white corresponds to negative values and dark grey to positive values.

corresponding to this length scale. On the other hand, the distribution of the a species shows a shorter characteristic length scale that is autonomously ge density-dependent social behavior. More difficult to discern in the density distri evident in the associated power spectra (Figure 6b), is the result that the large-sca in the density distribution of the aggregating species is nearly unchanged from purely diffusing species. Substantial changes in the spectra, however, occur at h numbers (i.e., small scales), where the addition of aggregating behavior to dispersing species increased the spectral energy at small length scales. Th qualitatively consistent with the trends observed in the empirical temperature, chlo krill biomass distributions.

*Conclusions*. The results of the spectral and wavelet analyses confir biomass distribution has more variability at small length scales than the dist temperature and chlorophyll, consistent with earlier investigations (Weber et al. et al. 1989). Wavelet analysis also demonstrated that krill had a multiscale pattern while temperature and chlorophyll had a single-scale pattern within the data resolution. The large-scale aggregations of krill (10 and 25 km range) ap composed of many small patches or swarms and were not the result of a diffuse, h aggregation of krill over a wide area. This implies that the mechanisms tha temperature and phytoplankton spatial patterns were different from those that con

The wavelet cross-covariance analyses indicated that temperature and chlo negatively correlated but spatially offset by some distance. One possible hypothes be explored based on this result is that the movement of cooler water masses at a km produces a corresponding 10 km sub-pattern in the phytoplankton comm cross-covariance of chlorophyll and krill spatial patterns also was negatively cc spatially offset. Grazing by krill may have contributed to the lack of cohere temperature and chlorophyll distributions. The field data (Figure 3) suggest a decrease in phytoplankton concentration, with the exception of the chlorophyl which occurred in the same location as the krill biomass minimum. The lack between chlorophyll and krill may also indicate that important scales of interac smaller than the sampling resolution or that complex interactions between biological processes obscure the mechanisms.

Nevertheless, the numerous small patches of krill within larger aggr evidence of the importance of social behavior to small-scale variability. The im this behavior are demonstrated by the model. Although the model tremendous the true behavior of Antarctic krill in a complex, three-dimensional environme used to show some important properties of the spectra of schooling and swarm First, the aggregations that result from this type of behavior are resistant to velocity perturbations (such as those present in turbulence) when the length aggregation is up to an order of magnitude larger than the sensing dista aggregations are characterized by high variability at small length scales. Thus, behavior can account for, in principle, the observed increase of krill spectral den length scales relative to those of a passively convected scalar.

Second, at length scales much larger (several orders of magnitude) thar distance, aggregations resulting from density-dependent behavior have very litt At large length scales, the distribution patterns are determined by the external adv even when the characteristic external velocity is small compared to the

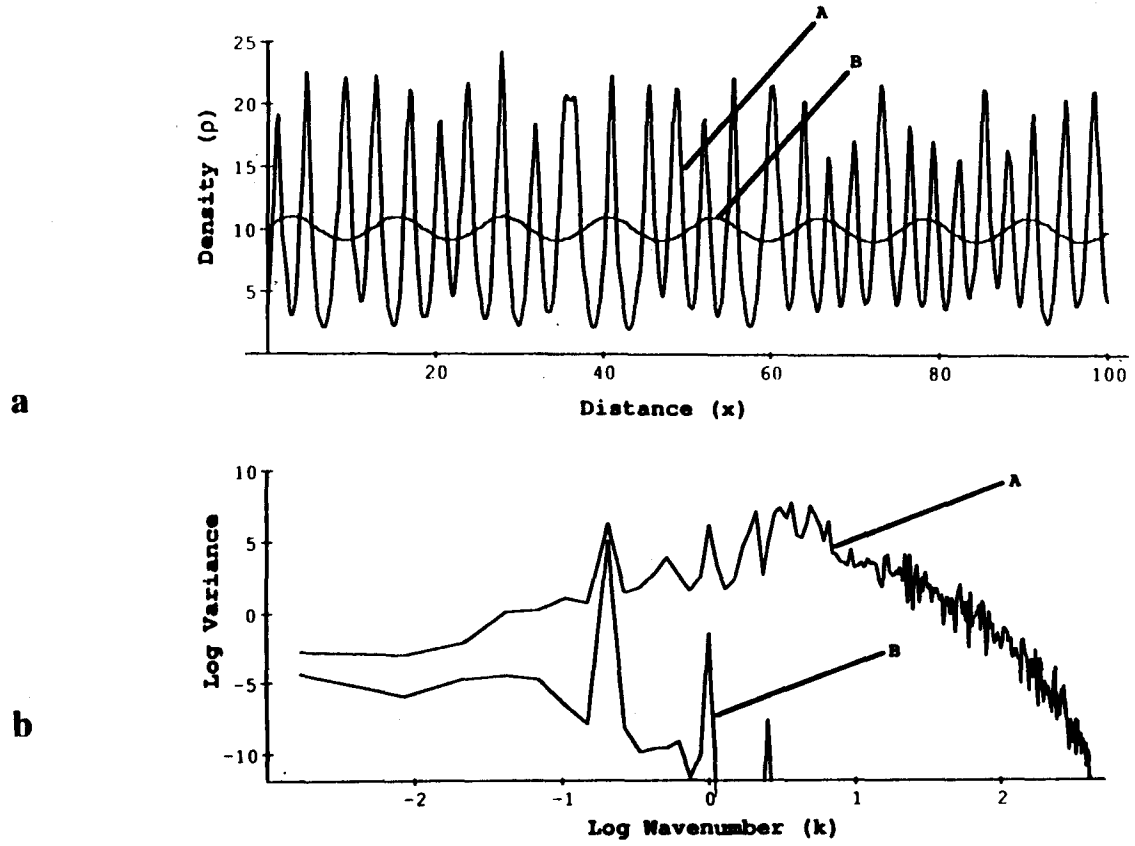


Figure 6. (a) Plots of population density vs. distance for aggregating (A) and non-aggregating (B) species in an environment with a continuous forcing velocity field of the form $v(x,t) = v_o \sin(k_o(x - ct))$. The advection parameters are $v_o = 0.5$, $k_o = 0.16\,n$, and $c = 0.05$. The diffusion coefficient, aggregation velocity, and target density are $D = 0.25$, $\tau = 0.3535$, and $\mu = 20$, respectively. (b) Power spectra (log-log plots) for density distributions of the aggregating (A) and non-aggregating (B) species in Figure 6a. The peak in both plots at wave number $k = -0.688$ corresponds directly to the sinusoidal forcing frequency. At higher wave numbers, the pure diffusion case (B) shows some additional energy peaks at subharmonics of the forcing frequency, while aggregation behavior (A) leads to significantly higher variability.

aggregation velocities of individuals. Hence, the effect of aggregation behavior on spectra density is strongly length-scale specific: the model predicts an approximate length-scal threshold, below which distribution is determined by social behavior and above whic distribution derives from physical oceanographic processes.

These preliminary results illustrate the benefits of a combined analytical and empirica approach to studying pattern-generating mechanisms. Both statistical analyses of field dat and theoretical modeling suggest that behavior may be more important than physical processe in determining meso-scale spatial patterns of krill. A number of underlying mechanisms ma produce similar spatial patterns; hence, an investigation of an ecosystem must combin knowledge about the spatial distribution patterns of physical and biological variables wit experimental and theoretical studies.

## PATCH FORMATION AS A RESULT OF THE COUPLING OF DIFFERENT MECHANISMS

The interplay of time and space is central to patch dynamics. A variety of nonlinear syster when extended into space are capable of a rich range of possible dynamics (Crutchfield an Kaneko 1987). In ecology, the study of such systems remains an open area. The next tw models illustrate the complex spatiotemporal patterns generated by predator-prey interactior when coupled by dispersal.

### Diffusion-Induced Chaos or Quasiperiodicity in a Spatial Predator-Prey System

Ecologists have long appreciated the role of diffusion as a pattern generator. In his classic work on morphogenesis, Turing (1952) first demonstrated the somewhat paradoxical notic that diffusion may lead to instability and spatial pattern. Segel and Jackson (1972) and Lev and Segel (1976) introduced diffusion instability into ecology as a mechanism for generatir patchiness in homogeneous environments. In heterogeneous environments, diffusion has bee generally viewed as a stabilizing influence (Comins and Blatt 1974, McMurtie 1978). Tl following work argues against such a view. We explore a mechanism for generatir patchiness involving the interplay of diffusion, predator-prey cycles, and a spatial gradien The model demonstrates that diffusion can lead to complex patterns of variability by spatial coupling local predator-prey cycles of different frequencies. Preliminary results suggest th the spatial distributions of predator and prey are chaotic or quasiperiodic in time.

*Model description.* The problem was posed in its simplest form by modelir predator-prey interactions in one-dimensional space. Both species diffuse at the same rate $l$ along a spatial gradient. Environmental heterogeneity is introduced by letting the pr intrinsic growth rate $R$ vary linearly with space. Let $P(X,T)$ and $H(X,T)$ denote, respectivel the prey and predator numbers at location $X$ and time $T$. Assume a logistic growth rate of tl prey and a Type II saturating functional response of the predator. Then, the followir equations describe the predator-prey dynamics in time and space:

$$\frac{\partial P}{\partial T} = RP(1-\frac{P}{K}) - \frac{bC_1P}{C_2+P}H + D_0\frac{\partial^2 P}{\partial X^2}$$
$$\frac{\partial H}{\partial T} = \frac{C_1P}{C_2+P}H - d_0H + D_0\frac{\partial^2 H}{\partial X^2} \qquad (1)$$

The parameters $K$, $d_0$, and $^1/_b$ denote the carrying capacity of the prey, the death rate of the predator, and the conversion rate of prey ingested to predator growth, respectively. The constants $C_1$ and $C_2$ set the parameters for the saturating functional response.

Also, no flux is assumed at the boundaries, and hence, at $X = 0$ and $X = L$,

$$\frac{\partial P}{\partial X} = \frac{\partial H}{\partial X} = 0$$

With the dimensionless variables $p = P/K$, $h = bH/K$, $x = X/L$, and $t = RT$ where $R = R(X_0)$ for some $X_0$ in $(0,L)$, system (1) becomes

$$\frac{\partial p}{\partial t} = rp(1-p) - \frac{Ap}{1+Bp}h + D\frac{\partial^2 p}{\partial x^2}$$
$$\frac{\partial h}{\partial t} = \frac{Ap}{1+Bp}h - dh + D\frac{\partial^2 h}{\partial x^2} \qquad (2)$$

where

$$r(x) = \frac{R}{\bar{R}} = m + nx, \quad A = \frac{C_1K}{C_2\bar{R}}, \quad B = \frac{K}{C_2}, \quad d = \frac{d_0}{\bar{R}}, \quad D = \frac{D_0}{L^2\bar{R}}.$$

At the boundaries, $x = 0$ and $x = 1$

$$\frac{\partial p}{\partial x} = \frac{\partial h}{\partial x} = 0$$

The dynamics of system (2) were investigated numerically with a finite difference integration scheme using 100 spatial grid sites.

*Results*. The following results illustrate the dynamics of equations (2) for a single parameter set (A = 5, B = 5, d = 0.6, m = 1.8 and n = -1.4), chosen to obtain limit cycles at each fixed location along the gradient in the absence of diffusion. When diffusion is added, $D = 10^{-4}$, the system exhibits sharply different dynamics. Changes in behavior occur in both space and time (Figures 7a,b,c), and trajectories show sensitivity to initial conditions. The resulting spatial distributions of both species along the gradient are then aperiodic, either quasiperiodic or chaotic in time.

Hence, diffusion may yield an asymptotic state that changes continuously in space and time. A synoptic observer would then see patches changing continuously in form and location (Figure 8). Preliminary exploration of the parameter space reveals that complex dynamics occur only at intermediate values of the diffusion rate. Also, as the diffusion rate is decreased, the transition to temporal chaos may occur through a quasiperiodic route (Schaffer 1988). The steepness of the environmental gradient also plays a critical role. At the limit of a uniform environment, cycles are again the rule. We are presently working on a more definite characterization of the dynamics of the system.

*Conclusions.* Predator-prey systems, by virtue of their nonlinearity, are known to exhibit complex dynamics. Previous work has focused on the temporal interplay of oscillations (Gilpin 1979, Hastings and Powell 1991, Kot et al. 1991). These preliminary results add the spatial dimension and show that diffusion may drive an otherwise periodic predator-prey system into aperiodic behavior. Vastano et al. (1990) describe a similar phenomenon for a chemical system. Kot (1989) demonstrates that diffusion can lead to period-doubling bifurcation and chaos in discrete predator-prey models. However, these models are already capable of complex dynamics with no added spatial dimension. We have presented a mechanism that in spite of its simplicity creates a dynamic patchiness in the distributions of predator and prey.

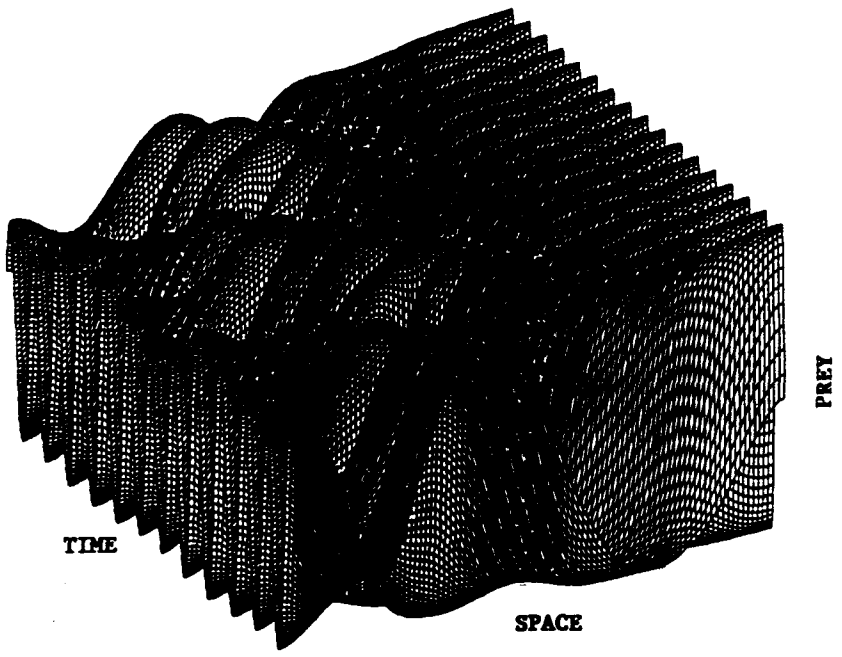


Figure 8. Spatiotemporal variation in prey numbers.

## Dispersal of a Predator and Its Prey in a Two-Dimensional Spatial Grid

Environmental heterogeneity can function as an external or induced mechanism generatin patchy distributions of organisms (Kareiva 1990, Doak et al. in press, Hilborn 1975 Robinson and Quinn 1988). Behavioral strategies that promote aggregation can be expecte to create clumpy distributions of individuals in homogeneous landscapes (Grünbaum, 1991) such behavior would typify an internal or autonomous mechanism. However, the presenc of non-uniform distributions of species need not imply the existence of such explicit patch forming mechanisms are at work. In this section, a model is presented in which randor movement, in the form of dispersal, interacting with a predator-prey model, leads to th generation of patchy distributions of individuals in a landscape consisting of discrete but equa patches.

*Model description.* The model consists of a two-dimensional square array of cells Every cell in the array can support a fixed population of a prey species; i.e., a carryin capacity for the cells is defined. In addition, a predator species can exist in each cell. At an one time, a cell is classified as being in one of four possible states: empty, only prey presen only predators present, and both prey and predator present. Because the predator cannot exi in the absence of prey, the state with only predators is necessarily considered to be transien Cells in the array are linked through the dispersal of both the prey and the predator species The array that we used for this investigation was 50 x 50 cells and had wrapping boundar conditions.

Each time the model was run, initial numbers of prey and predators were randoml distributed throughout the array. From then on, the predator and prey populations in eac cell were governed by a density-dependent Nicholson-Bailey model (Hassell 1976). Th model used was:

$$N_{t+1} = N_t \exp\left[r\left(1 - \frac{N_t}{K}\right) - aP_t\right]$$

$$P_{t+1} = \alpha N_t\{1 - \exp[-aP_t]\}$$

where $N$ indicates the prey and $P$ the predator. If the population of either species fell to les than one-half (in one cell), it was truncated to zero. Spatial interactions were defined b specifying maximum step sizes for both species, and by fixing the fraction of each populatio that dispersed from a cell at every time step. The fraction dispersing was the same for eac cell (though not necessarily the same for prey and predator), and dispersing individuals move in a random direction a distance ranging between zero and their maximum step size. A ste of size one would take an individual to one of its 8 nearest neighbors, and so on for large movements. No cost (e.g., increased mortality) was associated with dispersal. All disperser successfully arrived at a given cell (dispersal to and from the same cell was allowed). Mode dynamics were explored by changing the fraction of predators that dispersed (from 0.05 t 0.15) while holding other parameters fixed. The other parameters used for each model ru were: fraction of prey that disperse = 0.01; prey maximum step size = 1; predato maximum step size = 5; $r = 2$, $K = 100$, $a = 0.5$, and $\alpha = 1.00$. In a single cell, thes parameters led to the predators' eliminating the prey in a relatively short time.

To investigate further the dynamics of the spatial predator-prey system, a patch-counting algorithm was constructed. A patch was defined as any collection of cells that were connected by sides or corners. The inclusion of patches connected only by a corner is consistent with our dispersal mechanism as described above. This design eliminates the bias toward orthogonal directions that is otherwise present in grid models. The patch-counting algorithm was used to generate a frequency distribution of patch sizes. Each frequency distribution was constructed by allowing the model to run for 100 time steps to eliminate transient effects. Then, prey patches, consisting of cells with prey or cells with predators and prey, were counted for 750 subsequent time steps. The shape of the patch frequency distribution became fully expressed after at most 500 steps.

*Results*. The limiting distribution of prey and predators was quite sensitive to the rate at which predators dispersed. The distribution of prey appears increasingly clumpy as the fraction of dispersing predators grows (Figure 9). The mean numbers of prey and predators decrease as the predator dispersal rate increases. However, the predators were unable to persist if significantly less than 5% dispersed. Predators would eliminate the prey in their vicinity and then die off before finding new patches. At 15% predator dispersal, the prey were frequently reduced nearly to zero, which would precipitate a crash of the predator population. Large outbreaks of prey were common in this scenario, as a few cells always escaped the onslaught and managed to grow into large new patches before the predator population recovered. Predator dispersal rates greater than 15% led to a complete extermination of the prey.

Patch frequencies resulting from a completely random process were also generated. When the Nicholson-Bailey model was run, the number of grid cells containing prey was tabulated for every step. A patch size distribution for a random process was then obtained by placing an equal number of cells randomly throughout the array for the same number of steps and counting up the patches that resulted. This was done to allow the frequency distributions obtained from the Nicholson-Bailey model to be contrasted with those obtained from a random placement of cells.

The "envelopes" that contained the patch size distributions for the Nicholson-Bailey and the random process model runs are outlined to facilitate inspection (Figure 10). The distributions for the two processes represent the same total number of cells of prey in each case. A sudden loss of large patches of prey takes place as the fraction of predators dispersing increases from 5% to 9%. The presence of large patches of prey when 5% of the predators disperse can be explained in part by a tendency for percolating networks to form as the number of cells containing prey increases in a grid of fixed size. Applications from results of percolation theory suggest that, as the frequency of cells of one type grows, the likelihood that extremely large clusters of these cells will form increases dramatically (Gardner and O'Neill 1991). With this model, the effect of predator dispersal reaches a threshold at around 8%, and beyond this percolating networks rapidly disappear.

As the fraction of dispersing predators increases, the Nicholson-Bailey patch size distribution deviates from that of a random process (Figure 10). The average number of cells containing prey declines rapidly as predator dispersal grows, and this is reflected in the patch size distribution for the random process containing increasing numbers of patches in the range of 1 to 10, with the difference made up in diminishing numbers of large patches. The shape of the Nicholson-Bailey patch size distribution changes abruptly at the ends of the range of dispersal parameters investigated, and more smoothly in the middle.

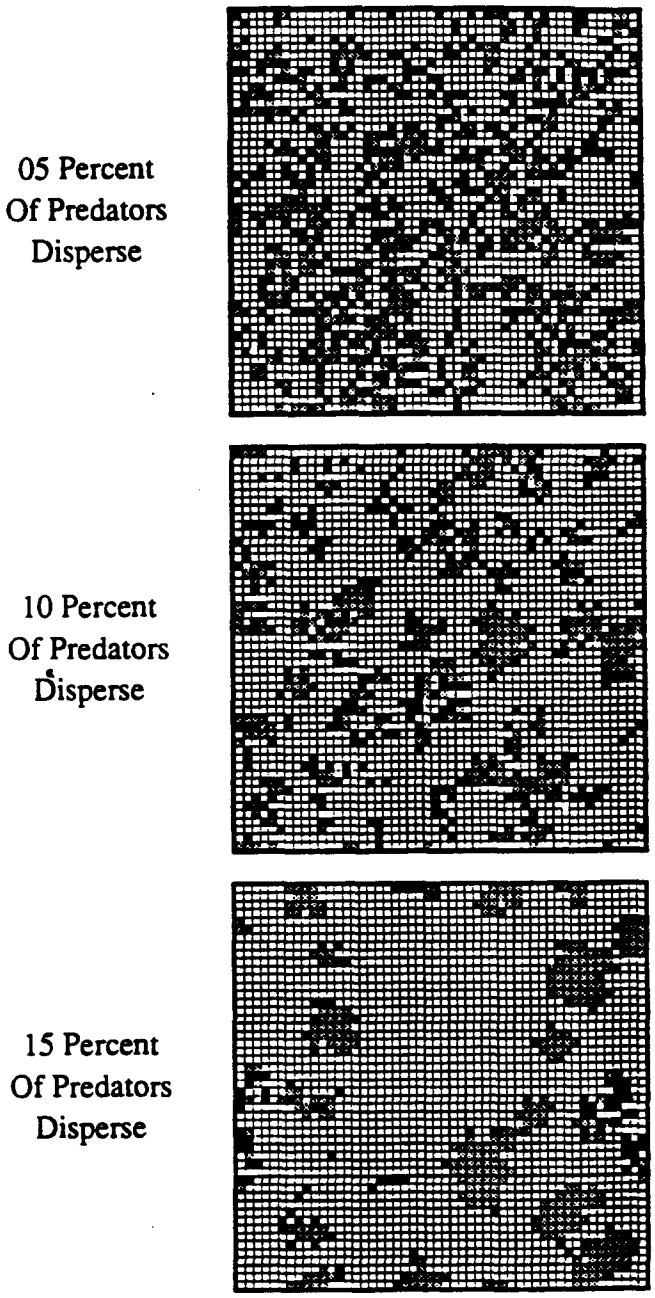


Figure 9. Snapshots in time of the array of cells for three different fractions of predators dispersing. Grey cells contain only the prey species and black cells contain both prey and predators. Empty cells have neither prey nor predators in them. The value of 10% predator dispersal was not used in the model runs, but is displayed here for clarity of presentation. The grid is 50 x 50 cells.

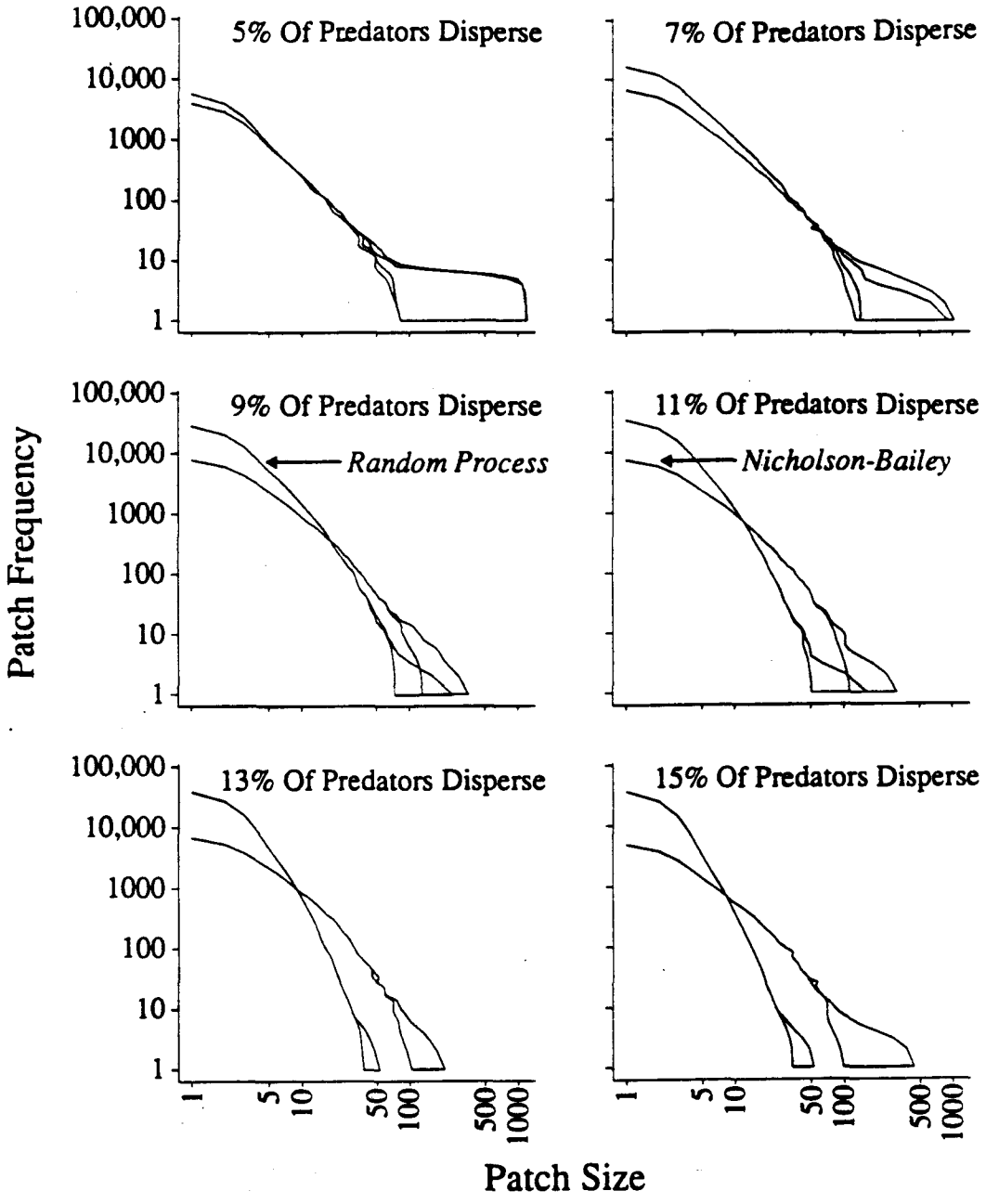


Figure 10. Envelopes containing the patch size distributions for the Nicholson-Bailey and random process models. All of the data points fell within the regions plotted in the figure, and the envelopes were drawn so that overlapping areas could be seen more clearly. Each graph corresponds to a different fraction of predators dispersing.

In a limited sense, the degree to which the distribution of prey is patchy can be thought of as a measure of its deviation from a random distribution. To illustrate the extent to which the spatial arrangement of prey deviated from that of a random distribution, we subtracted the random patch frequency distributions from the corresponding Nicholson-Bailey distributions (Figure 11). Our intent in this analysis was to focus on the tendency for increased clumping of prey in the spatial Nicholson-Bailey model over that of a random process, and thus only the portions of the graphs greater than zero were plotted in this figure. The enhancement of a narrow region of the patch distribution as a result of the dispersal process can be clearly seen. The deviation from the random distribution is greatest in the intermediate patch sizes, and these data serve to quantify the notion of patch generation invoked from the series of plots (see Figure 9). The decrease in the height of the maximum in Figure 11, as the fraction of predators dispersing grows from 13% to 15%, is due to a sudden increase in the maximum patch size. This phenomenon results from the large prey outbreaks that occur when 15% of the predators disperse.

*Conclusions.* Results from this model suggest that random movements of prey and predators in a uniform landscape can generate a highly non-random spatial distribution of the prey species. The degree to which the distribution of prey was non-random was shown to be a function of the number of predators that dispersed. Further, an approach has been outlined with which these spatial distributions can be quantified and the results used to enhance a definition of patchiness.

This work was carried out and the section was written before the work by Hassell et al. (1991) was published. They have shown that a system similar to the one presented here is capable of generating spatial chaos.

## CONCLUDING REMARKS

By definition, patch dynamics combines the temporal and the spatial dimensions. The explicit consideration of space leads to the explicit consideration of the environment, such as the transport of organisms by the physics in the ocean. Dichotomies such as physical vs. biological, or induced vs. autonomous, have developed in attempts to classify mechanisms of patch formation. However, a focus on the interaction between the environment and the organisms at different spatial scales would lead to a better understanding of patch dynamics. It is imperative that ecologists avoid arbitrarily selected scales for empirical and theoretical research. The scaling of patches and their complex interactions between mechanisms and across scales remain as obstacles to our understanding. Once we have broadened our understanding of these processes, we can begin to make meaningful comparisons of mechanisms across organisms and ecosystems. The collection of projects in this chapter explore this idea.

## ACKNOWLEDGMENTS

This chapter has benefitted from discussions with many of the participants in the Patch Dynamics Workshop. In particular, we wish to thank Simon Levin, Tom Powell, and John Steele, Graciela García-Moliner, and Pablo Marquet. This chapter also was improved by comments from Jonathon Dushoff and Mary Schumacher.

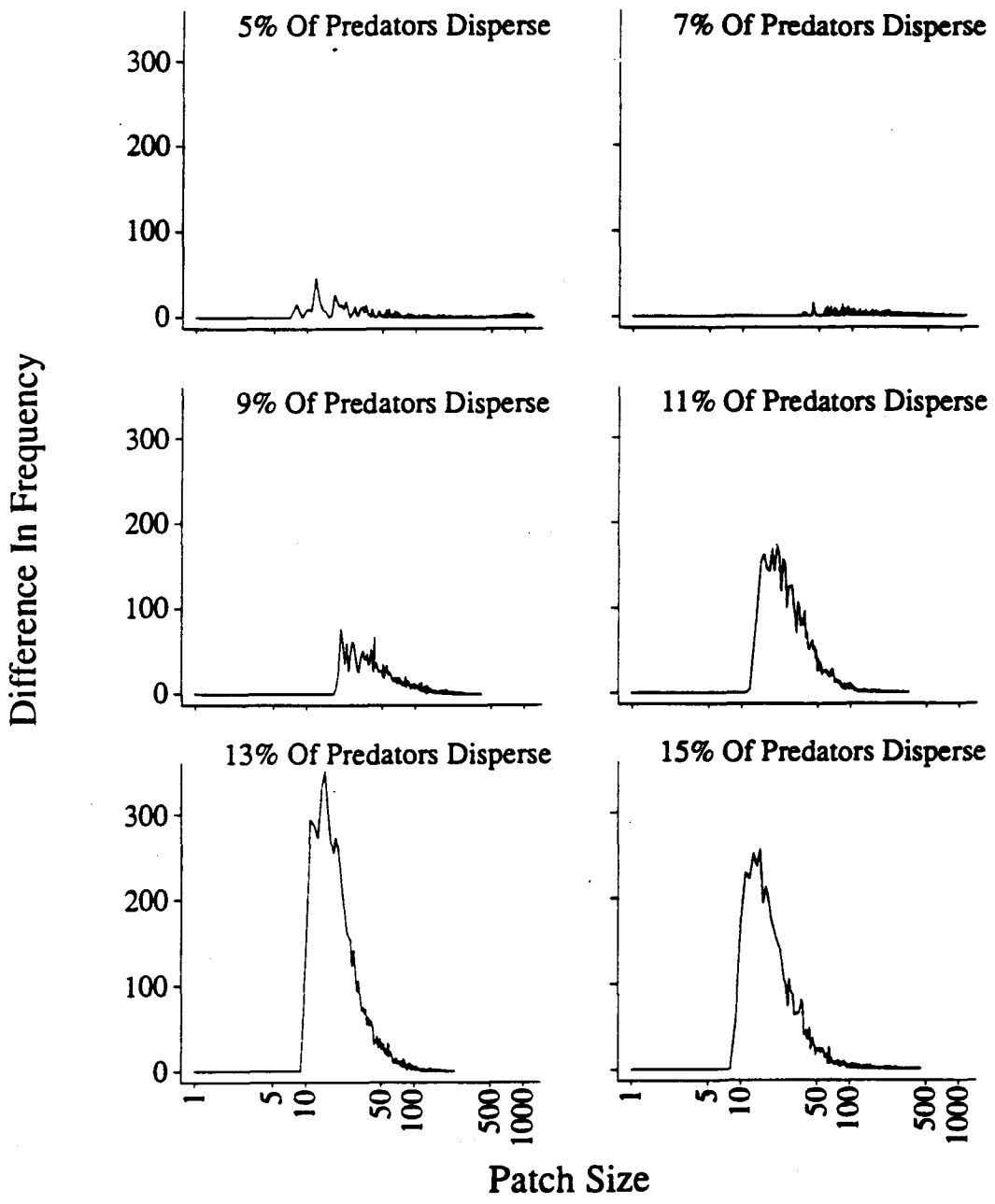


Figure 11. The amount by which the Nicolson-Bailey patch size distribution exceeded the random distribution. This graph was generated by subtracting the frequency distributions for the random process from those of the Nicolson-Bailey process in Figure 10 (when the random distribution exceeded the Nicholson-Bailey distribution, the results were set to zero). Each graph corresponds to a different fraction of predators dispersing.

## REFERENCES


Addicott, J. F., J. M. Aho, M. F. Antolin, D. K. Padilla, J. S. Richardson and D. A. Soluk. 198 Ecological neighborhoods: Scaling environmental patterns. *Oikos* 49:340-346.

Argoul, F., A. Arneodo, G. Grasseau, Y. Gagne, E. J. Hopfinger, and U. Frisch. 1989. Wavelet analysis turbulence reveals the multi-fractal nature of the Richardson cascade. *Nature* 338:51-53.

Bradshaw, G. A. 1991. Analysis of hierarchical pattern and process in Douglas-fir forests using wave analysis. Ph. D. dissertation, Oregon State University, Corvallis, OR.

Bradshaw, G. A., and T. A. Spies. In press. Characterizing canopy gap structure in forests using the wave transform. *J. Ecol.*

Comins, H. N., and D. W. E. Blatt. 1974. Prey-predator models in spatially heterogenous environments. *Theor. Biol.* 48:75-83.

Crutchfield, J. P., and K. Kaneko. 1987. Phenomenology of spatio-temporal chaos. In: H. Bai-L *Directions in Chaos*. World Scientific Publishing, Singapore. pp. 272-353.

Daly, K. L., and M. C. Macaulay. 1991. The influence of physical and biological mesoscale dynamics on seasonal distribution and behavior of *Euphausia superba* Dana in the Antarctic marginal ice zone. *M Ecol. Prog. Ser.* 79:37-66.

Doak D., P. Marino, and P. M. Kareiva. In Press. Spatial scale mediates the influence of hab fragmentation on dispersal success: Implications for conservation. *Theor. Popul. Biol.*

Downes, B. J. 1990. Patch dynamics and mobility of fauna in streams and other habitats. *Oikos* 59:411-4

Gardner, R. H., and R. V. O'Neill. 1991. Pattern, process, and predictability: The use of neutral models landscape analysis. In: M. G. Turner and R. H. Gardner (eds.). *Quantitative Methods in Landsc Ecology*. Springer-Verlag, New York, NY, pp. 289-307.

Gilpin, M. E. 1979. Spiral chaos in a predator-prey model. *Am. Nat.* 107:306-308.

Grünbaum, D. 1991. Three unrelated projects in mathematical biology. Ph. D. dissertation, Cor University, Ithaca, NY.

Hassell, M. P. 1976. Arthropod predator-prey systems. In: R. M. May (ed.). *Theoretical Ecology: Princi and Applications* - 2nd ed. Sinauer Associates, Inc., Sunderland, MA, pp. 105-131.

Hassell, M. P., H. N. Comins, and R. M. May. 1991. Spatial structure and chaos in insect popula dynamics. *Nature* 353:255-258.

Hastings, A., and T. Powell. 1991. Chaos in a three-species food chain. *Ecology* 72(3):896-903.

Haury, L. R., J. A. McGowan, and P. H. Wiebe. 1978. Patterns and processes in the time-space scale plankton distributions. In: J. H. Steele (ed.). *Spatial Pattern in Plankton Communities*. Plenum Pr New York, pp. 277-327.

Hilborn R. 1975. The effect of spatial heterogeneity on the persistence of predator-prey interactions. *Th Popul. Biol.* 8(3):346-355

Hutchinson, G. E. 1961. The paradox of the plankton. *Am. Nat.* 95:137-145.

Kareiva, P. 1990. Population dynamics in spatially complex environments: Theory and data. *Philos. Tr R. Soc. London*, Ser. B 330:175-190.

Kolasa, J., and S. Pickett (eds). 1991. *Ecological Heterogeneity*. Springer-Verlag, New York.

Kot, M. 1989. Diffusion-driven period-doubling bifurcations. *BioSystems* 22:279-287.

Kot, M., G. S. Sayler, and T. W. Schultz. In press. Complex dynamics in a model microbial system. *I Math. Biol.*

Kotliar, N. B., and J. A. Wiens. 1990. Multiple scales of patchiness and patch structure: A hierarcl framework for the study of heterogeneity. *Oikos* 59:253-260.

Levin, S. A., A. Morin, and T. M. Powell. 1989. Patterns and processes in the distribution and dynamic Antarctic krill. CCAMLR Scient. Rep. VII/BG/20:281-296.

Levin, S. A., and R. T. Paine. 1974. Disturbance, patch formation and community structure. *Proc. Acad. Sci. USA* 71(7):2744-2747.

Levin, S., and L. A. Segel. 1976. Hypothesis for origin of planktonic patchiness. *Nature* 259:659.

Mackas, D. C., K. L. Denman, and M. R. Abbott. 1985. Plankton patchiness: Biology in the phy vernacular. *Bull. Mar. Sci.* 37:652-674.

McMurtie, R. 1978. Persistence and stability of single-species and prey-predator systems in spat heterogeneous environments. *Math. Biosci.* 39:11-51.

Milne, B. T. 1991. Renormalization relations for spatial models. Paper presented at the Annual Meeting, Ecological Society of America, San Antonio, TX.

Platt, T., and K. L. Denman. 1975. Spectral analysis in ecology. *Ann. Rev. Ecol. Syst.* 6:189-210.

Pickett, S. T. A., and P. S. White (eds). 1985. *The Ecology of Natural Disturbances and Patch Dynamics.* Academic Press, San Diego, CA.

Price, H. J., K. R. Boyd, and C. M. Boyd. 1988. Omnivorous feeding behavior of the Antarctic krill *Euphausia superba*. *Mar. Biol.* 97:67-77.

Robinson G. R., and J. F. Quinn. 1988. Extinction, turnover and species diversity in an experimentally fragmented California (USA) grassland. *Oecologia* (Berlin) 76:71-86.

Rosenberg, J. and R. Hewitt. 1991. AMLR 1990/1991 field season report, Objectives, accomplishments and tentative conclusions. Administrative report LJ-91-18, NOAA/NMFS/Southwest Fisheries Science Center, La Jolla, California.

Roughgarden, J. 1977. Patchiness in the spatial distribution of a population caused by stochastic fluctuations in resources. *Oikos* 29:52-59.

Sahrhage, D. 1988. Summary and conclusions. In: D. Sahrhage, (ed.). *Antarctic Ocean and Resources Variability.* Springer-Verlag, Berlin, pp. 297-300.

Schaffer, W. M. 1988. Perceiving order in the chaos of nature. In: M. S. Boyce (ed.). *Evolution of Life Histories of Mammals: Theory and Pattern.* Yale University Press, New Haven and London, pp. 313-350.

Segel, L. A., and J. L. Jackson. 1972. Dissipative structure: An explanation and an ecological example. *J. Theor. Biol.* 37:545-559.

Steele, J. H. 1978. Some comments on plankton patches. In: J. H. Steele (ed.). *Spatial Pattern in Plankton Communities.* Plenum Press, New York, pp. 1-20.

Stommel, H. 1963. Varieties of oceanographic experience. *Science* 139:572-576.

Turing, A. M. 1952. The chemical basis of morphogenesis. *Philos. Trans. R. Soc. London*, Ser. B 237:37-72.

Vastano, J. A., T. Russo, and H. L. Swinney. 1990. Bifurcation to spatially induced chaos in a reaction-diffusion system. *Physica D* 46:23-42.

Weber, L. H., S. Z. El-Sayed, and I. Hampton. 1986. The variance spectra of phytoplankton, krill and water temperature in the Antarctic Ocean south of Africa. *Deep-Sea Res.* 33:1327-1343.

Wiens, J. A. 1976. Population responses to patchy environments. *Ann. Rev. of Ecol. Syst.* 7:81-120.

Wiens, J. A., and B. T. Milne. 1989. Scaling of 'landscapes' in landscape ecology, or landscape ecology from a beetle's perspective. *Landscape Ecology* 3:87-96.